IEEE Access
Multidisciplinary ⋮ Rapid Review ⋮ Open Access Journal

Received 15 July 2023, accepted 31 July 2023, date of publication 3 August 2023, date of current version 9 August 2023.

*Digital Object Identifier 10.1109/ACCESS.2023.3301562*

RESEARCH ARTICLE

# Brain-Inspired Mutual Synchronization in Cross-Coupled $NbO_x$ Oscillation Neurons for Oscillatory Neural Network Applications

**HYUN WOOK KIM[1], (Graduate Student Member, IEEE), SEYEONG JEON[2], SEONUK JEON[1], (Graduate Student Member, IEEE), EUNRYEONG HONG[1], (Graduate Student Member, IEEE), NAYEON KIM[1], (Graduate Student Member, IEEE), AND JIYONG WOO[1], (Associate Member, IEEE)**

[1]School of Electronic and Electrical Engineering, Kyungpook National University, Daegu 41566, South Korea
[2]School of Mechanical Engineering, Ulsan National Institute of Science and Technology, Ulsan 44919, South Korea

Corresponding author: Jiyong Woo (jiyong.woo@knu.ac.kr)

This work was supported in part by the National Research Foundation (NRF) funded by the Korean Government [Ministry of Science and ICT (MSIT)], South Korea, under Grant NRF-2021R1C1C1003261; in part by MSIT under the Information Technology Research Center (ITRC) of Program Supervised by the Institute for Information and Communications Technology Planning and Evaluation (IITP) under Grant IITP-2022-RS-2022-00156225; in part by the National Research and Development Program through the NRF of Korea funded by MSIT under Grant 2020M3H2A1078045, and in part by the Technology Innovation Program (or Industrial Strategic Technology Development Program) funded by the Ministry of Trade, Industry and Energy (MOTIE, Korea) under Grant RS-2023-00231956 and Grant 1415187475.

**ABSTRACT** The brain performs cognitive functions through rhythmic communications of neural oscillations across numerous spatially distributed neurons. This process is known as ''binding by synchrony''. Herein, we demonstrate oscillatory neural networks (ONNs) based on a nanoscale $NbO_x$ device for compact oscillation neurons (ONs). When a voltage ($V_{DD}$) is applied to the $NbO_x$-based device, a high resistance state is temporarily changed to a low resistance state due to the formation of a conducting path. Owing to the volatile switching characteristics, the $V_{DD}$ across the $NbO_x$ device, serially connected with an additional load resistor ($R_L$), is repeatedly increased and decreased, generating oscillations at the intermediate node. We experimentally investigated the impact of $R_L$ and $V_{DD}$ on the oscillation behavior of the single ON circuit. Thereafter, through simulations, we analyzed the interactions between the voltage oscillations when two $NbO_x$-based ONs were connected by a coupling element (e.g., variable resistor or capacitor). The results showed that the oscillations were either in- or out-of-phase synchronized owing to the coupling strength. These two distinguishable synchronizations can be used to encode binary information in the phase domain, resulting in energy-efficient computing. This study proves that by building ONNs comprising multiple ONs, both sharp edges and pretrained patterns can be detected from images.

**INDEX TERMS** $NbO_x$-based device, oscillation neurons, oscillatory neural networks, pattern recognition.

## I. INTRODUCTION

The development of artificial intelligence algorithms has enabled machines to perform natural language translation and pattern recognition [1], [2], [3], [4]. This has led to a dramatic increase in the number of parameters and datasets used in applications, implying the need for data-centric computing. Conventional computing systems based on the von Neumann architecture work by sequentially loading data across the memory elements and processing units [5], [6], [7], [8], [9]. As the amount of data increases exponentially, the performance gains are limited by delays in the data transfer process. Therefore, neuromorphic technologies emulating the biological structure of the brain have recently attracted considerable attention. The brain comprises nearly 100 billion crosslinked neurons, which communicate by exchanging

The associate editor coordinating the review of this manuscript and approving it for publication was Ye Zhou.

neuronal signals through synapses [10], [11]. Therefore, fully parallel computing enhances the efficiency of a brain system, and many studies have attempted to implement parallel structures for synapses using cross-point resistive memory arrays [12], [13]. In addition, recent studies have shown associative memory by developing analog circuits that describe the integrate-and-fire behavior of neurons [14], [15], [16].

As neuroscience has further explored the underlying principles of the brain, the mechanisms of cognitive tasks performed by collective behavior of neurons that are widely dispersed in brain have been elucidated. Neurons generate their own signal oscillations, and the interacting signals are eventually synchronized, resulting in a perceptron function [17]. Based on this understanding, the use of oscillatory neural networks (ONNs), wherein all artificial neurons are connected, has been demonstrated in various image processing techniques [18], [19]. For neuron devices that can generate continuous oscillations, nano-oscillators have been studied instead of the conventional oscillator circuits composed of many transistors [18], [19], [20], [21]. Threshold switching devices based on binary oxide or chalcogenide materials have primarily been used as oscillation neurons (ONs). When the voltage applied to the threshold switching device exceeds the threshold voltage ($V_{TH}$), the high resistance state changes to a low resistance state. When the voltage is lower than the hold voltage ($V_{HOLD}$), the changed state rapidly returns to the initial state. In a circuit configuration wherein the threshold switching device is connected to an additional load resistor ($R_L$), a continuous voltage oscillation with a specific frequency is generated at the intermediate node [22], [23], [24], [25].

In this study, we developed $NbO_x$-based threshold switching devices for ONs and conducted experiments and simulation studies to identify the natural responses of oscillations in different environments. More specifically, reliable voltage oscillation was first achieved in a single ON circuit through device characterization, and the oscillation tunability was determined as a function of the $R_L$ and applied voltage pulse ($V_{DD}$). Subsequently, a simulation was used to investigate the mutual synchronization of oscillations in ONN systems, wherein multiple ONs are cross-coupled, for edge detection and image recognition tasks.

## II. MATERIALS AND METHODS

Reactive sputtering was used to deposit a 50-nm-thick $NbO_x$ layer on top of a plug-type TiN bottom electrode having a diameter of 30 nm. Subsequently, a TiN-based top electrode of size $10 \times 10\ \mu m^2$ was patterned using photolithography. The performance of the fabricated $NbO_x$-based ON device was evaluated by applying $V_{DD}$ to the top electrode and grounding the bottom electrode using an HP 4156C semiconductor parameter analyzer. An Agilent 81110A pulse generator was used for the oscillation measurements, and the response of the ON device was detected using a Keysight CX3300 current waveform analyzer.

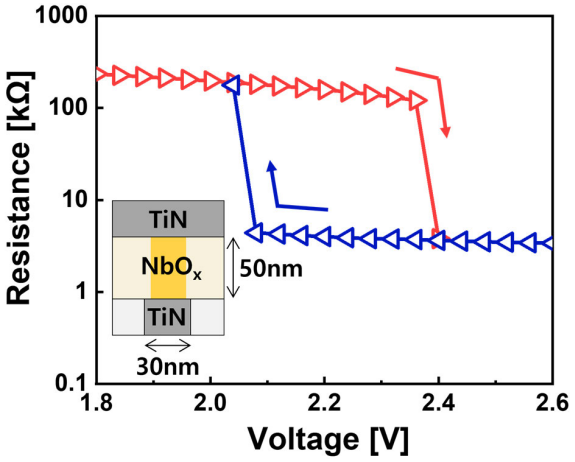


**FIGURE 1.** Resistance–voltage curve of the fabricated threshold switching device comprising a TiN/$NbO_x$/TiN stack.

## III. RESULTS AND DISCUSSION

### A. SINGLE ON DEVICE

The fabricated threshold switching device exhibited two volatile resistance states, as shown in Fig. 1 [22]. As voltage was applied, a high resistance of hundreds of kΩ was abruptly converted to a low resistance of several kΩ at a $V_{TH}$ of approximately 2.4 V. In contrast, a voltage lower than $V_{HOLD}$ of 2.1 V caused the low resistance state to return to its initial state. This threshold switching has been explained by the nucleation theory [26]. The electric field induced the agglomeration of oxygen vacancies in the $NbO_x$ layer, thus creating a conductive path. This locally formed path was thermodynamically stable only when a voltage was applied, and it dissolved spontaneously when the voltage was removed.

For the ON element, the $NbO_x$ device was connected in series with the $R_L$, as shown in Fig. 2a. A $V_{DD}$ with a pulse width of 50 $\mu$s was provided through the pulse generator, and the intermediate node between the $R_L$ and $NbO_x$-based ON was monitored using the analyzer. In general, the initial high resistance of the ON device was larger than that of the $R_L$. Most of the $V_{DD}$ was first applied to the ON, which increased the output voltage ($V_{out}$) at the intermediate node. When the ON device was turned on, the $V_{DD}$ began transferring to the $R_L$, causing $V_{out}$ to decrease. Therefore, the $NbO_x$-based ON device was repeatedly turned on and off at a given $V_{DD}$, resulting in $V_{out}$ oscillations. Because charging/discharging dynamics play an important role in triggering the oscillations, designing an appropriate $R_L$ range can help achieve robust oscillation behavior. As shown in Fig. 2b, the single ON device produced oscillations with a frequency of approximately 670 kHz; however, random $V_{out}$ spikes were observed. This is because the resistance of the $NbO_x$ device at the $V_{HOLD}$ can be lower than that of the $R_L$ owing to device variability, thereby preventing dynamics. Reliable $V_{out}$ oscillations were observed when $R_L > 3.9$ kΩ was used, as shown in Figs. 2c and 2d. The frequency was inversely proportional to $R_L$, as shown in Fig. 2e.

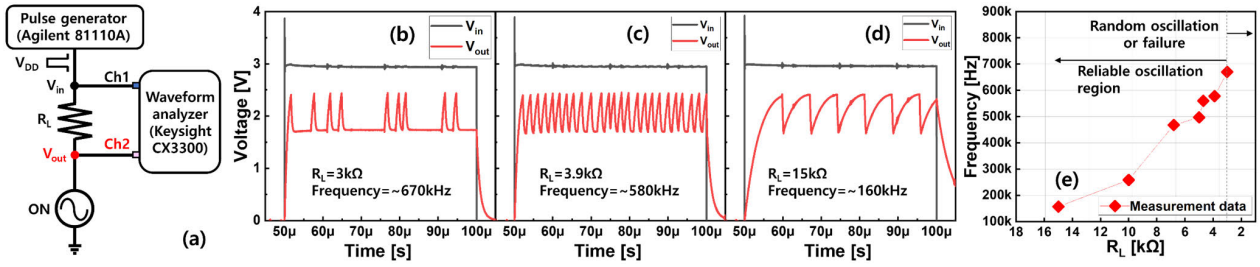


**FIGURE 2.** (a) Schematic of the single ON circuit, where the $NbO_x$-based ON device is connected using the $R_L$. The $V_{DD}$ was provided from the pulse generator, and the signals were evaluated through the waveform analyzer. $V_{out}$ oscillations for $R_L$ stacks of (b) 3 kΩ, (c) 3.9 kΩ, and (d) 15 kΩ. (e) Faster frequency obtained by lowering the $R_L$ stack.

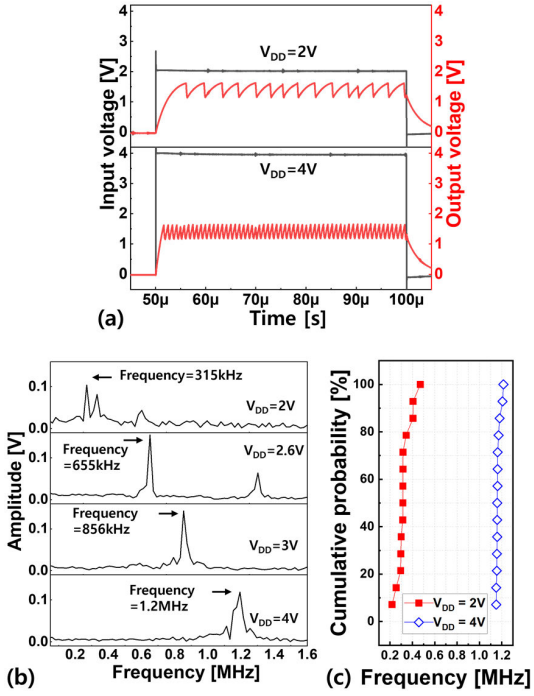


**FIGURE 3.** (a) $V_{out}$ oscillation of the single $NbO_x$-based ON device as a function of $V_{DD}$. (b) Faster oscillation frequency extracted from the fast Fourier transform obtained owing to the higher $V_{DD}$. (c) In addition to the faster frequency, a more uniform frequency distribution during the oscillation was achieved at $V_{DD}$ of 4 V.

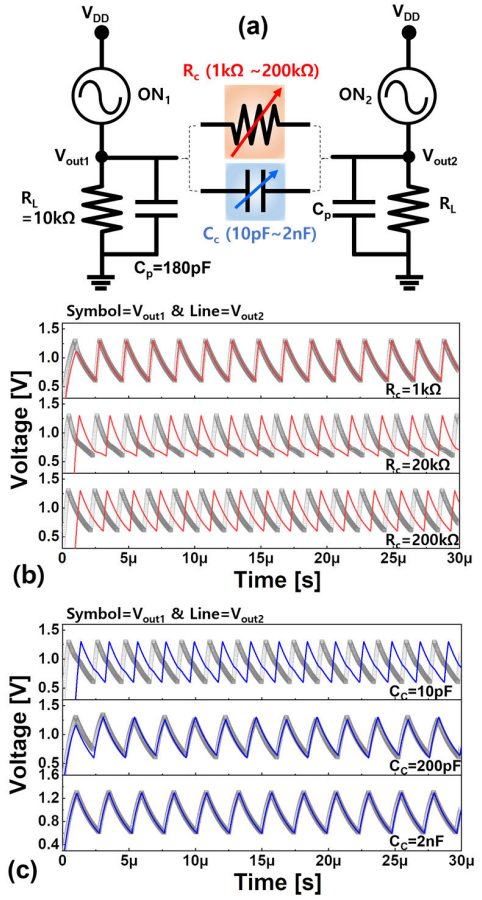


**FIGURE 4.** (a) Schematic of the coupled $NbO_x$-ONs. The HSPICE simulation results show that the synchronization of the two oscillations was achieved differently as a function of the type of coupling element and its strength. (b) Lowering $R_c$ resulted in in-phase synchronization. (c) In-phase synchronization was obtained as the $C_c$ was increased.

Further, we investigated the effect of $V_{DD}$ on the oscillation frequency. Because $V_{DD}$ was greater than the $V_{TH}$ of the $NbO_x$-based ON, $V_{out}$ oscillations could be achieved. To analyze the oscillation response over a wide range of $V_{DD}$, a threshold switching device with a $V_{TH}$ of less than 2 V was used, which was fabricated using a thinner $NbO_x$ layer [22]. The higher the $V_{DD}$, the faster the frequency, as shown in Fig. 3a. The peak frequency was extracted through fast Fourier transform, as shown in Fig. 3b. By increasing $V_{DD}$ from 2 to 4 V, the location of the maximum frequency amplitude moved from 315 kHz to 1.2 MHz. A tight distribution of each frequency was also obtained using a larger $V_{DD}$, as shown in Fig. 3c. These results indicate that the $V_{out}$ oscillation can be tuned using both the operating voltage conditions and the internal controllable components (e.g., $R_L$).

### B. COUPLED ON DEVICES

To understand the interaction of $V_{out}$ oscillations in coupled $NbO_x$-based ONs, we performed HSPICE simulations using the measurement data. Two identical $NbO_x$-based ONs were coupled using a variable resistor (or capacitor), as shown in Fig. 4a. We assumed an $R_L$ of 10 kΩ and a parasitic capacitance ($C_p$) of 180 pF. $V_{out}$ for the left and right ON elements were defined as $V_{out1}$ and $V_{out2}$, respectively. The $V_{out1}$ oscillation ("symbol" curve) of the $ON_1$ was activated,

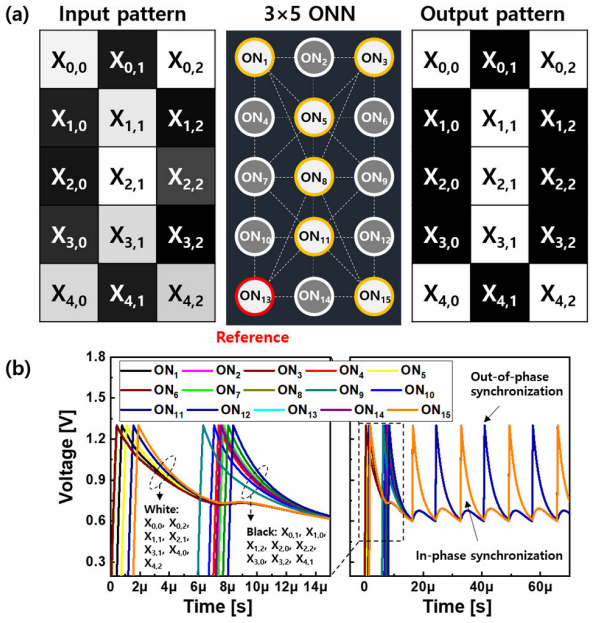


**FIGURE 5.** (a) Input pattern can be recognized in the 3 × 5 ONN. (b) All oscillation responses obtained from the ONN system under the given noisy zero pattern. The data from the magnified region (<20 $\mu$s) clearly show individual oscillations based on pixel colors. The oscillations are synchronized over time, and two synchronization methods can be observed.

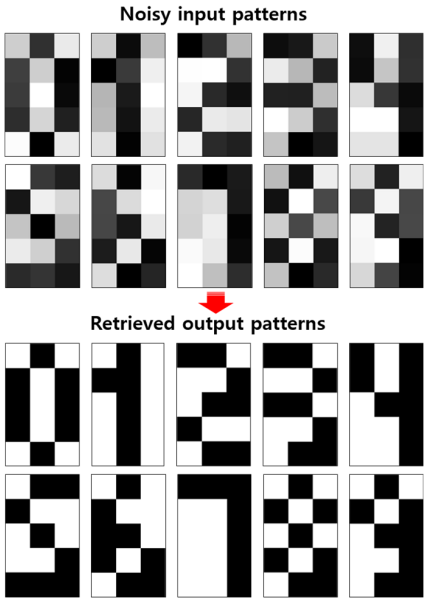


**FIGURE 6.** ONN accurately identified the noisy input patterns (expressed in gray in pixels).

as shown in Fig. 4b. Unlike the single oscillation circuit configuration for electrical measurements, the $R_L$ was connected to ground in simulations. The position where the $R_L$ is connected induces a change in the order in which charging/discharging occurs, so the oscillation frequency is the same [22], [24]. To examine the effect of the coupling strength, $V_{DD}$ with a slight delay was applied to $ON_2$. When the $NbO_x$-based ONs were strongly connected with a smaller coupling resistance ($R_c$) of 1 k$\Omega$, the $V_{out1}$ and $V_{out2}$ oscillations rapidly became similar, resulting in in-phase synchronization. A larger $R_c$ of 20 k$\Omega$ caused the $V_{out2}$ oscillation ("line" curve) to steadily shift toward the right, implying quasi out-of-phase synchronization. Out-of-phase synchronization was eventually exhibited when two ONs with $R_c$ of 200 k$\Omega$ were connected. This indicates that the weak coupling of the coupled ONs induces oscillation phase inversion [27], [28]. However, when a variable capacitor was employed as the coupling component, the voltages of the two ONs were shared, thereby mitigating the voltage difference. A larger coupling capacitance ($C_c$) of 2 nF induced a longer voltage-sharing time, allowing sufficient time for the $V_{out}$ oscillation to achieve in-phase synchronization, as shown in Fig. 4c. The voltage-sharing time was shortened using a smaller $C_c$ of 10 pF. The voltage difference at each ON was still noticeable; thus, out-of-phase synchronization was preferred.

### C. ONN SYSTEMS

For neural network applications, an ONN comprising 15 ONs was built using MATLAB/Simulink [29]. Because all ONs were fully connected through $R_c$, the Hebbian learning rule was used to map the $R_c$ values of the 3 × 5 digit patterns, as shown in Fig. 5a [30], [31], [32]. A 3 × 5 ONN that corresponded to each pixel of the input pattern was constructed. Thus, trained weights were assigned to each $R_c$ in the ONN. The pixel color of the input pattern was classified using the $V_{DD}$ delay entering the ONN system, which was determined based on the degree of darkness. The $V_{DD}$ of the brightest white pixel was applied to ON device immediately without any delay to trigger oscillation. Compared to this pixel, the darker pixels produced a $V_{DD}$ with a delay. The ONN systems utilized how oscillations that turn on at different times interact and synchronize to distinguish patterns [28]. ONs corresponding to brighter pixel positions exhibited oscillations within 2 $\mu$s, as shown in Fig. 5b. In contrast, the oscillations of the ONs representing darker pixels were activated after ~6 $\mu$s. The oscillation of an ON that was strongly (or weakly) coupled to neighboring ONs naturally converged into in-phase (or out-of-phase) synchronization. Consequently, the random oscillations in the initial stage were soon converted into one of two phases: 0° or 180°. This implies that even noisy patterns could be clearly retrieved (Fig. 6), which is useful for hardware security applications and pattern recognition tasks [33].

The ONN can also serve as a convolutional filter for detecting edges within an image, as shown in Fig. 7. Many recent studies have attempted to implement filtering algorithms on hardware using cross-point resistive memory arrays [34], [35]. The convolutional output is determined by sensing the weighted sum current along a specific column in the array, which consumes power. Instead, when a 3 × 3 ONN filter scans an image to find matches with pretrained horizontal, vertical, and diagonal patterns, the ONN system drives the oscillations in an out-of-phase synchronization [19]. The

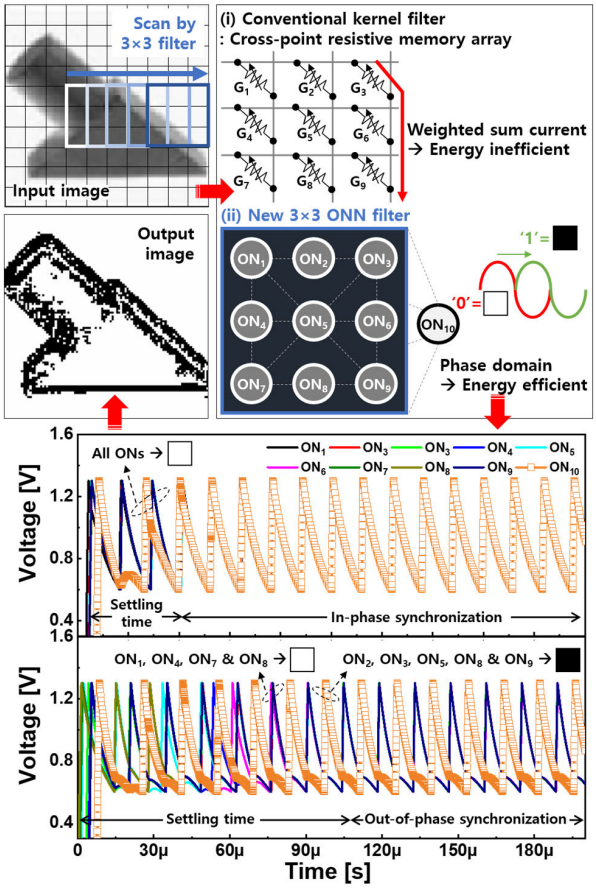


**FIGURE 7.** Input image scanned using the 3 × 3 ONN filter. The nine oscillations were synchronized based on the scanned patterns. The out-of-phase synchronization was observed only when the trained patterns were detected, allowing for extraction of the edges of the image.

output color was extracted through comparisons with the reference ON, which is denoted as $ON_{10}$ in this study. In a 100 × 100 image obtained from the Columbia Object Image Library, areas without dark colors showed in-phase synchronization after the settling time, which were represented by white pixels. When one of the three patterns was detected during scanning, the oscillations of the specific ONs preferred to interact in an out-of-phase synchronization.

These results indicated that ONN systems implemented by densely integrated $NbO_x$-based ONs in a limited space instead of conventional neuron circuits composed of multiple transistors can demonstrate a compact image processing chip. Furthermore, the ONN systems encoding the output information in the phase domain rather than the current (or voltage) are expected to reduce energy consumption [19].

## IV. CONCLUSION

We examined the $V_{out}$ oscillation behavior of the fabricated nanoscale $NbO_x$-based ON as a function of $R_L$ and $V_{DD}$. We revealed that in image-processing applications, the $V_{out}$ oscillations are linked based on the strength of the coupling element, resulting in two types of synchronizations. Thus, the black and white color ranges of a given image are clearly classified as either white or black, allowing ONN systems to perform pattern recognition and edge detection using the given hardware.

## REFERENCES


[1] D. Kuzum, S. Yu, and H. S. P. Wong, "Synaptic electronics: Materials, devices and applications," *Nanotechnology*, vol. 24, no. 38, pp. 1–23, Sep. 2013, doi: 10.1088/0957-4484/24/38/382001.

[2] S. Seo, S.-H. Jo, S. Kim, J. Shim, S. Oh, J.-H. Kim, K. Heo, J.-W. Choi, C. Choi, S. Oh, D. Kuzum, H.-S.-P. Wong, and J.-H. Park, "Artificial optic-neural synapse for colored and color-mixed pattern recognition," *Nature Commun.*, vol. 9, no. 1, p. 5106, Nov. 2018, doi: 10.1038/s41467-018-07572-5.

[3] K. Roy, A. Jaiswal, and P. Panda, "Towards spike-based machine intelligence with neuromorphic computing," *Nature*, vol. 575, no. 7784, pp. 607–617, Nov. 2019, doi: 10.1038/s41586-019-1677-2.

[4] G. W. Burr, R. M. Shelby, A. Sebastian, S. Kim, S. Kim, S. Sidler, K. Virwani, M. Ishii, P. Narayanan, A. Fumarola, L. L. Sanches, I. Boybat, M. L. Gallo, K. Moon, J. Woo, H. Hwang, and Y. Leblebici, "Neuromorphic computing using non-volatile memory," *Adv. Phys. X*, vol. 2, no. 1, pp. 89–124, Jan. 2017, doi: 10.1080/23746149.2016.1259585.

[5] D. Ielmini and H.-S.-P. Wong, "In-memory computing with resistive switching devices," *Nature Electron.*, vol. 1, no. 6, pp. 333–343, Jun. 2018, doi: 10.1038/s41928-018-0092-2.

[6] W. Zhang, B. Gao, J. Tang, P. Yao, S. Yu, M.-F. Chang, H.-J. Yoo, H. Qian, and H. Wu, "Neuro-inspired computing chips," *Nature Electron.*, vol. 3, no. 7, pp. 371–382, Jul. 2020, doi: 10.1038/s41928-020-0435-7.

[7] Q. Xia and J. J. Yang, "Memristive crossbar arrays for brain-inspired computing," *Nature Mater.*, vol. 18, no. 4, pp. 309–323, Mar. 2019, doi: 10.1038/s41563-019-0291-x.

[8] M. Hu, C. E. Graves, C. Li, Y. Li, N. Ge, E. Montgomery, N. Davila, H. Jiang, R. S. Williams, J. J. Yang, Q. Xia, and J. P. Strachan, "Memristor-based analog computation and neural network classification with a dot product engine," *Adv. Mater.*, vol. 30, no. 9, pp. 1–10, Jan. 2018, doi: 10.1002/adma.201705914.

[9] H. Yeon, P. Lin, C. Choi, S. H. Tan, Y. Park, D. Lee, J. Lee, F. Xu, B. Gao, H. Wu, H. Qian, Y. Nie, S. Kim, and J. Kim, "Alloying conducting channels for reliable neuromorphic computing," *Nature Nanotechnol.*, vol. 15, no. 7, pp. 574–579, Jul. 2020, doi: 10.1038/s41565-020-0694-5.

[10] N. Qiao, H. Mostafa, F. Corradi, M. Osswald, F. Stefanini, D. Sumislawska, and G. Indiveri, "A reconfigurable on-line learning spiking neuromorphic processor comprising 256 neurons and 128K synapses," *Frontiers Neurosci.*, vol. 9, p. 141, Apr. 2015, doi: 10.3389/fnins.2015.00141.

[11] I. Boybat, M. L. Gallo, S. R. Nandakumar, T. Moraitis, T. Parnell, T. Tuma, B. Rajendran, Y. Leblebici, A. Sebastian, and E. Eleftheriou, "Neuromorphic computing with multi-memristive synapses," *Nature Commun.*, vol. 9, no. 1, p. 2514, Jun. 2018, doi: 10.1038/s41467-018-04933-y.

[12] W. Wan, R. Kubendran, C. Schaefer, S. B. Eryilmaz, W. Zhang, D. Wu, S. Deiss, P. Raina, H. Qian, B. Gao, S. Joshi, H. Wu, H.-S.-P. Wong, and G. Cauwenberghs, "A compute-in-memory chip based on resistive random-access memory," *Nature*, vol. 608, no. 7923, pp. 504–512, Aug. 2022, doi: 10.1038/s41586-022-04992-8.

[13] J. Woo, K. Moon, J. Song, S. Lee, M. Kwak, J. Park, and H. Hwang, "Improved synaptic behavior under identical pulses using $AlO_x/HfO_2$ bilayer RRAM array for neuromorphic systems," *IEEE Electron Device Lett.*, vol. 37, no. 8, pp. 994–997, Aug. 2016, doi: 10.1109/LED.2016.2582859.

[14] J. Sun, Y. Wang, P. Liu, S. Wen, and Y. Wang, "Memristor-based neural network circuit with multimode generalization and differentiation on Pavlov associative memory," *IEEE Trans. Cybern.*, vol. 53, no. 5, pp. 3351–3362, May 2023, doi: 10.1109/TCYB.2022.3200751.

[15] Q. Xu, Y. Wang, B. Chen, Z. Li, and N. Wang, "Firing pattern in a memristive Hodgkin–Huxley circuit: Numerical simulation and analog circuit validation," *Chaos, Solitons Fractals*, vol. 172, pp. 1–10, Jul. 2023, doi: 10.1016/j.chaos.2023.113627.

[16] J. Sun, Y. Wang, P. Liu, and S. Wen, "Memristor-based circuit design of PAD emotional space and its application in mood congruity," *IEEE Internet Things J.*, early access, Apr. 18, 2023, doi: 10.1109/JIOT.2023.3267778.

[17] P. Uhlhaas, "Neural synchrony in cortical networks: History, concept and current status," *Frontiers Integrative Neurosci.*, vol. 3, p. 17, Jul. 2009, doi: 10.3389/neuro.07.017.2009.

[18] C. Delacour and A. Todri-Sanial, "Mapping Hebbian learning rules to coupling resistances for oscillatory neural networks," *Frontiers Neurosci.*, vol. 15, Nov. 2021, Art. no. 694549, doi: 10.3389/fnins.2021.694549.
[19] C. Dealcour, S. Carapezzi, M. Abernot, and A. Todri-Sanial, "Energy-performance assessment of oscillatory neural networks based on $VO_2$ devices for future edge AI computing," *IEEE Trans. Neural Netw. Learn. Syst.*, early access, Jan. 26, 2023, doi: 10.1109/TNNLS.2023.3238473.
[20] M. Romera, P. Talatchian, S. Tsunegi, K. Yakushiji, A. Fukushima, H. Kubota, S. Yuasa, V. Cros, P. Bortolotti, M. Ernoult, D. Querlioz, and J. Grollier, "Binding events through the mutual synchronization of spintronic nano-neurons," *Nature Commun.*, vol. 13, no. 1, p. 883, Feb. 2022, doi: 10.1038/s41467-022-28159-1.
[21] N. Shukla, W. Y. Tsai, M. Jerry, M. Barth, V. Narayanan, and S. Datta, "Ultra low power coupled oscillator arrays for computer vision applications," in *Proc. IEEE Symp. VLSI Technol.*, Jun. 2016, pp. 1–2, doi: 10.1109/VLSIT.2016.7573439.
[22] H. W. Kim, H. Kang, E. Hong, and J. Woo, "Area and thickness scaling of $NbO_x$-based threshold switches for oscillation neurons," *IEEE J. Electron Devices Soc.*, vol. 10, pp. 397–401, 2022, doi: 10.1109/JEDS.2022.3169745.
[23] P. Wang, A. I. Khan, and S. Yu, "Cryogenic behavior of $NbO_2$ based threshold switching devices as oscillation neurons," *Appl. Phys. Lett.*, vol. 116, no. 16, Apr. 2020, Art. no. 162108, doi: 10.1063/5.0006467.
[24] L. Gao, P.-Y. Chen, and S. Yu, "$NbO_x$ based oscillation neuron for neuromorphic computing," *Appl. Phys. Lett.*, vol. 111, no. 10, Sep. 2017, Art. no. 103503, doi: 10.1063/1.4991917.
[25] D. Lee, J. Lee, S. Lee, C. Lee, S. Heo, and H. Hwang, "Nonvolatile frequency-programmable oscillator with $NbO_2$ and Li-based electrochemical random access memory for coupled oscillators-based temporal pattern recognition system," *IEEE Electron Device Lett.*, vol. 43, no. 7, pp. 1041–1044, Jul. 2022, doi: 10.1109/LED.2022.3172124.
[26] S. Lee, J. Yoo, J. Park, and H. Hwang, "Understanding of the abrupt resistive transition in different types of threshold switching devices from materials perspective," *IEEE Trans. Electron Devices*, vol. 67, no. 7, pp. 2878–2883, Jul. 2020, doi: 10.1109/TED.2020.2997670.
[27] M. Wickramasinghe and I. Z. Kiss, "Synchronization of electrochemical oscillators with differential coupling," *Phys. Rev. E, Stat. Phys. Plasmas Fluids Relat. Interdiscip. Top.*, vol. 88, no. 6, Dec. 2013, Art. no. 062911, doi: 10.1103/PhysRevE.88.062911.
[28] E. Corti, A. Khanna, K. Niang, J. Robertson, K. E. Moselund, B. Gotsmann, S. Datta, and S. Karg, "Time-delay encoded image recognition in a network of resistively coupled $VO_2$ on Si oscillators," *IEEE Electron Device Lett.*, vol. 41, no. 4, pp. 629–632, Apr. 2020, doi: 10.1109/LED.2020.2972006.
[29] H. W. Kim, S. Jeon, H. Kang, E. Hong, N. Kim, and J. Woo, "Understanding rhythmic synchronization of oscillatory neural networks based on $NbO_x$ artificial neurons for edge detection," *IEEE Trans. Electron Devices*, vol. 70, no. 6, pp. 3031–3036, Jun. 2023, doi: 10.1109/TED.2023.3263818.
[30] S. Carapezzi, G. Boschetto, C. Delacour, E. Corti, A. Plews, A. Nejim, S. Karg, and A. Todri-Sanial, "Advanced design methods from materials and devices to circuits for brain-inspired oscillatory neural networks for edge computing," *IEEE J. Emerg. Sel. Topics Circuits Syst.*, vol. 11, no. 4, pp. 586–596, Dec. 2021, doi: 10.1109/JETCAS.2021.3128756.
[31] J. Núñez, M. J. Avedillo, M. Jiménez, J. M. Quintana, A. Todri-Sanial, E. Corti, S. Karg, and B. Linares-Barranco, "Oscillatory neural networks using $VO_2$ based phase encoded logic," *Frontiers Neurosci.*, vol. 15, Apr. 2021, Art. no. 655823, doi: 10.3389/fnins.2021.655823.
[32] M. Abernot, T. Gil, M. Jiménez, J. Núñez, M. J. Avellido, B. Linares-Barranco, T. Gonos, T. Hardelin, and A. Todri-Sanial, "Digital implementation of oscillatory neural network for image recognition applications," *Frontiers Neurosci.*, vol. 15, Aug. 2021, Art. no. 713054, doi: 10.3389/fnins.2021.713054.
[33] A. Todri-Sanial, S. Carapezzi, C. Delacour, M. Abernot, T. Gil, E. Corti, S. F. Karg, J. Nüñez, M. Jiménèz, M. J. Avedillo, and B. Linares-Barranco, "How frequency injection locking can train oscillatory neural networks to compute in phase," *IEEE Trans. Neural Netw. Learn. Syst.*, vol. 33, no. 5, pp. 1996–2009, May 2022, doi: 10.1109/TNNLS.2021.3107771.
[34] L. Gao, P.-Y. Chen, and S. Yu, "Demonstration of convolution kernel operation on resistive cross-point array," *IEEE Electron Device Lett.*, vol. 37, no. 7, pp. 870–873, Jul. 2016, doi: 10.1109/LED.2016.2573140.
[35] E. Hong, S. Jeon, N. Kim, H. W. Kim, H. Kang, K. Moon, and J. Woo, "Convolutional kernel with $PrCaMnO_x$-based resistive random-access memory for neuromorphic image processing," *AIP Adv.*, vol. 13, no. 1, Jan. 2023, Art. no. 015318, doi: 10.1063/5.0133846.

**HYUN WOOK KIM** (Graduate Student Member, IEEE) received the B.S. degree in electronics engineering from Kyungpook National University, Daegu, Republic of Korea, in 2022, where he is currently pursuing the M.S. degree in electronic and electrical engineering.

**SEYEONG JEON** received the B.S. degree in mechanical engineering from the Ulsan National Institute of Science and Technology, Ulsan, Republic of Korea, in 2021.

**SEONUK JEON** (Graduate Student Member, IEEE) received the B.S. degree in electronics engineering from Kyungpook National University, Daegu, Republic of Korea, in 2023, where he is currently pursuing the M.S. degree in electronic and electrical engineering.

**EUNRYEONG HONG** (Graduate Student Member, IEEE) received the B.S. degree in electronics engineering from Kyungpook National University, Daegu, Republic of Korea, in 2022, where she is currently pursuing the M.S. degree in electronic and electrical engineering.

**NAYEON KIM** (Graduate Student Member, IEEE) received the B.S. degree in electronics engineering from Kyungpook National University, Daegu, Republic of Korea, in 2023, where she is currently pursuing the integrated B.S. and M.S. degree in electronic and electrical engineering.

**JIYONG WOO** (Associate Member, IEEE) received the Ph.D. degree in materials science and engineering from the Pohang University of Science and Technology, Pohang, South Korea, in 2017. He is currently an Assistant Professor in electronic and electrical engineering with Kyungpook National University, Daegu, Republic of Korea.